

The transcriptional co-regulator LDB1 is required for brown adipose function



Jessica D. Kepple^{1,2}, Yanping Liu^{1,2}, Teayoun Kim^{1,2}, Cheryl Cero⁴, James W. Johnson⁴, Glenn C. Rowe^{1,3}, Aaron M. Cypess⁴, Kirk M. Habegger^{1,2}, Martin Young^{1,3}, Chad S. Hunter^{1,2,*}

ABSTRACT

Objective: Brown adipose tissue (BAT) is critical for thermogenesis and glucose/lipid homeostasis. Exploiting the energy uncoupling capacity of BAT may reveal targets for obesity therapies. This exploitation requires a greater understanding of the transcriptional mechanisms underlying BAT function. One potential regulator of BAT is the transcriptional co-regulator LIM domain-binding protein 1 (LDB1), which acts as a dimerized scaffold, allowing for the assembly of transcriptional complexes. Utilizing a global LDB1 heterozygous mouse model, we recently reported that LDB1 might have novel roles in regulating BAT function. However, *direct* evidence for the LDB1 regulation of BAT thermogenesis and substrate utilization has not been elucidated. We hypothesize that brown adipocyte-expressed LDB1 is required for BAT function.

Methods: LDB1-deficient primary cells and brown adipocyte cell lines were assessed via qRT-PCR and western blotting for altered mRNA and protein levels to define the brown adipose-specific roles. We conducted chromatin immunoprecipitation with primary BAT tissue and immortalized cell lines. Potential transcriptional partners of LDB1 were revealed by conducting LIM factor surveys via qRT-PCR in mouse and human brown adipocytes. We developed a *Ucp1*-Cre-driven LDB1-deficiency mouse model, termed *Ldb1*^{ΔBAT}, to test LDB1 function *in vivo*. Glucose tolerance and uptake were assessed at thermoneutrality via intraperitoneal glucose challenge and glucose tracer studies. Insulin tolerance was measured at thermoneutrality and after stimulation with cold or the administration of the β3-adrenergic receptor (β3-AR) agonist CL316,243. Additionally, we analyzed plasma insulin via ELISA and insulin signaling via western blotting. Lipid metabolism was evaluated via BAT weight, histology, lipid droplet morphometry, and the examination of lipid-associated mRNA. Finally, energy expenditure and cold tolerance were evaluated via indirect calorimetry and cold challenges.

Results: Reducing *Ldb1* *in vitro* and *in vivo* resulted in altered BAT-selective mRNA, including *Ucp1*, *Elovl3*, and *Dio2*. In addition, there was reduced *Ucp1* induction *in vitro*. Impacts on gene expression may be due, in part, to LDB1 occupying *Ucp1* upstream regulatory domains. We also identified BAT-expressed LIM-domain factors *Lmo2*, *Lmo4*, and *Lhx8*, which may partner with LDB1 to mediate activity in brown adipocytes. Additionally, we observed *LDB1* enrichment in human brown adipose. *In vivo* analysis revealed LDB1 is required for whole-body glucose and insulin tolerance, in part through reduced glucose uptake into BAT. In *Ldb1*^{ΔBAT} tissue, we found significant alterations in insulin-signaling effectors. An assessment of brown adipocyte morphology and lipid droplet size revealed larger and more unilocular brown adipocytes in *Ldb1*^{ΔBAT} mice, particularly after a cold challenge. Alterations in lipid handling were further supported by reductions in mRNA associated with fatty acid oxidation and mitochondrial respiration. Finally, LDB1 is required for energy expenditure and cold tolerance in both male and female mice.

Conclusions: Our findings support LDB1 as a regulator of BAT function. Furthermore, given *LDB1* enrichment in human brown adipose, this co-regulator may have conserved roles in human BAT.

© 2021 The Author(s). Published by Elsevier GmbH. This is an open access article under the CC BY-NC-ND license (<http://creativecommons.org/licenses/by-nc-nd/4.0/>).

Keywords LDB1; Transcriptional co-regulator; Brown adipocyte; Thermogenesis; Glucose; Lipid; *Ucp1*

1. INTRODUCTION

Obesity contributes to metabolic dysregulation, including glucose intolerance and ectopic lipid deposition, ultimately affecting multiple organ systems. Brown adipose tissue (BAT) produces heat from stored energy and, thus, has potential as a novel therapeutic target for obesity-related diseases. Moreover, BAT expansion via transplantation or drug-induced stimulation improves glucose tolerance and insulin

sensitivity in rodent models [1–3]. BAT is present in adult humans and is activated by cold exposure, with BAT activity dampened in obese individuals [4,5]. These observations suggest that modulating BAT function is a potential therapeutic target against metabolic dysregulation.

Brown adipocytes are densely packed with mitochondria containing uncoupling protein-1 (UCP1), an inner membrane anion carrier that uncouples mitochondrial respiration, to dissipate energy as heat [6].

¹Comprehensive Diabetes Center and Department of Medicine, USA ²Division of Endocrinology, Diabetes and Metabolism, University of Alabama at Birmingham, Birmingham, AL, USA ³Division of Cardiovascular Diseases, Department of Medicine, University of Alabama at Birmingham, Birmingham, AL, USA ⁴Diabetes, Endocrinology, and Obesity Branch, Intramural Research Program, National Institute of Diabetes and Digestive and Kidney Diseases (NIDDK), NIH, Bethesda, MD, USA

*Corresponding author. 1825 University Boulevard, SHEL 1211, University of Alabama at Birmingham, Birmingham, AL 35294, USA. E-mail: huntercs@uab.edu (C.S. Hunter).

Received May 4, 2021 • Revision received June 22, 2021 • Accepted June 24, 2021 • Available online 29 June 2021

<https://doi.org/10.1016/j.molmet.2021.101284>

UCP1 is almost exclusively restricted to thermogenic adipose and is robustly increased by stimuli including cold exposure and a high-fat diet [6]. Global *Ucp1* deficiency results in cold intolerance and increased obesity susceptibility [7,8]. *Ucp1* expression and BAT function are regulated by transcriptional complexes comprised of transcription factors (TFs) and interacting transcriptional co-regulators [9]. However, many BAT TFs are also expressed in white adipocytes, placing greater importance on identifying BAT-enriched transcriptional co-regulators required for tissue-specific gene expression. Co-regulators, including PGC1 α and PRDM16, promote thermogenic gene expression by stabilizing complexes in the regulatory regions of brown adipocyte targets, including *Ucp1*. For example, PRDM16 is required for brown adipocyte development and function, and a loss of which results in cold intolerance and altered brown adipocyte identity, in part, through the reduced expression of genes that include *Ucp1*, *Cidea*, *Pgc1a*, and *Dio2* [10]. Though many TFs and co-regulators have been identified in brown adipocyte differentiation, the transcriptional complexes maintaining mature brown adipocyte function are not fully elucidated. A greater understanding of gene regulatory mechanisms governing normal brown adipose function will enhance the development of targeted therapies against metabolic dysregulation.

We previously identified LIM domain-binding protein 1 (LDB1) as a potential regulator of BAT function [11]. This co-regulator acts as a dimerized scaffold and directly binds LIM-domain factors, including LIM-domain TF and LIM-only (LMO) adaptor proteins [12]. *Ldb1* is widely expressed, including in BAT, and regulates metabolic function [11–13]. We assessed whole-body metabolism in global *Ldb1* heterozygous (i.e., *Ldb1*^{+/-}) lean and obese mice to determine how a mild genetic insult affects energy expenditure and glucose metabolism [11]. *Ldb1*^{+/-} mice displayed reduced energy expenditure at both ambient and reduced temperatures, suggesting thermogenic impairments. Thermogenic mRNAs, including *Elovl3*, involved in cellular lipid homeostasis, were reduced in *Ldb1*^{+/-} BAT. Chromatin immunoprecipitation (ChIP) analysis revealed LDB1 occupancy at an upstream *Elovl3* control domain, indicating LDB1 may directly regulate this BAT gene [11].

Due to the global LDB1 heterozygosity employed in our prior study, we could not assess the *direct* roles of BAT-expressed LDB1. Here, we examined the specific role of LDB1 as a novel effector of BAT function. *In vitro* experiments revealed *Ldb1*-deficient adipocytes had reduced BAT-selective mRNAs as well as adipogenic- and lipid-associated markers. Additionally, *Ldb1*-deficient adipocytes were unable to induce *Ucp1* expression upon β 3-AR agonism. Effects on *Ucp1* may be due, in part, to the LDB1 occupancy of *Ucp1* regulatory domains. Additionally, we found that BAT expresses several LIM-domain factors, which could serve as potential transcriptional partners mediating LDB1 action. *LDB1* expression was also enriched in human adipose biopsies, suggesting LDB1 may have analogous roles in humans. *In vivo* studies using a BAT-specific LDB1 knockout mouse model, termed *Ldb1* ^{Δ BAT}, revealed significant impacts on glucose and insulin tolerance. *Ldb1* ^{Δ BAT} mice had reduced BAT glucose uptake and altered lipid utilization, suggesting LDB1 regulates substrate metabolism in brown adipocytes. Finally, reductions in LDB1 resulted in significant impairments in thermogenesis and energy expenditure. Overall, our data support the regulatory importance of LDB1 in BAT function.

2. MATERIALS AND METHODS

2.1. Mice

All mice were fed a standard chow (4.7 kcal%, #7917, Envigo, Indianapolis, IN). The conditional BAT *Ldb1* knockout (*Ldb1* ^{Δ BAT}) model

was generated by crossing floxed *Ldb1* (*Ldb1*^{Flox}, defined as CTL) [14,15] and transgenic *Ucp1-Cre* mice (B6.FVB-Tg(*Ucp1-cre*)1Evdrl/J; Jax stock #024670) [16]. All mouse lines were maintained on a mixed (C57BL/6J) background. Mice were single- or group-housed on a 12 h:12 h light/dark cycle (lights on from 0600 to 1800 h) near thermoneutrality at 28 °C \pm 1 °C [17] and constant humidity with *ad libitum* access to food and water, except when noted. All studies were approved and performed according to the University of Alabama at Birmingham (UAB) Institutional Animal Care and Use Committee guidelines.

2.2. Stromal Vascular Fraction (SVF) induction and adenovirus transduction

The stromal vascular fraction containing preadipocytes was isolated from interscapular mouse BAT depots after dissection, mincing, collagenase digestion, and centrifugation [18]. The SVF pellet was resuspended in a maintenance media containing DMEM, fetal bovine serum, penicillin, and streptomycin (1% solution, Gibco by Life Technologies, # 15140-122) and seeded onto a 12-well dish. Adherent cells were switched to differentiation media (maintenance media supplemented with 20 nM insulin, 1 nM T3, 125 μ M indomethacin, 0.5 μ M dexamethasone, 0.5 mM IBMX, 5 μ M rosiglitazone) and cultured for up to 6 d, with feeding every 2 d. For the transduction of progenitors or mature brown adipocytes, adenovirus expressing LacZ or Cre was added to cultured *Ldb1*^{Flox} cells before induction at MOI = 10–100 (for 50,000 cells) for 48 h. A subset of cells was treated with the β 3-AR agonist [19] (CL316,243, 10 μ M, #50-476-10001 EMD Millipore/Calbiochem) or DMSO vehicle for 24 h.

2.3. Tissue isolation

Ad libitum-fed *Ldb1* ^{Δ BAT} and CTL *Ldb1*^{Flox} mice were anesthetized with isoflurane then euthanized via cervical dislocation. Tissues were harvested from brown, epididymal, and inguinal adipose deposits, flash-frozen, and stored at –80 °C until analysis. For the isolation and assessment of mature adipocytes, tissue was extracted, followed by collagenase digestion (Collagenase P, Roche, # 11249002001, 1.5 mg/ml) and centrifugation at 10,000 $\times g$ at 4 °C for 15 min. The top layer containing mature adipocytes was collected for analysis.

2.4. Cell lines

siRNA transfections [20] were conducted with the *Ucp1*-expressing X9 adipocyte cell line as previously described [21]. These cells were induced similarly to the SVF experiment detailed above. ChIP was performed using chromatin extracted from an immortalized brown preadipocyte cell line generously provided by Dr. Kai Ge (Adipocyte Biology and Gene Regulation Section, NIDDK) [22]. This cell line was also induced similarly to the SVF experiment detailed above.

2.5. Body composition and indirect calorimetry

Weekly body weights were collected on male and female CTL and *Ldb1* ^{Δ BAT} mice. Body composition was measured immediately before indirect calorimetry using noninvasive nuclear magnetic resonance spectroscopy (EchoMRI; Echo Medical Systems) at the UAB Nutrition Obesity Research Center Small Animal Phenotyping Core. The energy expenditure (EE), food intake, and respiratory quotient were simultaneously measured using a combined indirect calorimetry system (Comprehensive Laboratory Animal Monitoring System; Columbus Instruments) as previously described [11,23]. O₂ consumption and CO₂ production were measured every 15 min to determine the respiratory quotient and energy expenditure. Home-cage locomotor activity was determined using a multidimensional infrared light-beam system.

2.6. Western blotting

Western blotting was performed as described previously [20,24]. Polyvinylidene difluoride (PVDF) membranes were probed using the following primary antibodies: rabbit α -LDB1 (1:1000, generously provided by Dr. Paul Love, NIH), rabbit α -UCP1 (1:1000, Cell Signaling #14670S (D9D6X)), mouse α -Actin (1:1000, Abcam ab3280), rabbit α -pAKT^{S473} (1:1000, Cell Signaling #9271S), rabbit Pan AKT (1:3000, Cell Signaling #4691S), rabbit α -phospho-p44/42 MAPK^(T202/4204) (1:1000, Cell Signaling #4370S), and rabbit α -p44/42 MAPK^(T202/4204) (1:1000, Cell Signaling #4695S).

2.7. *In vivo* metabolic analysis

Mice underwent a 6-hour fast prior to intraperitoneal glucose tolerance tests (IPGTT) and intraperitoneal insulin tolerance tests (IPITT) as previously described [11,20]. Mice were then injected intraperitoneally with 2.0 g/kg body weight of glucose or 0.5 U/kg body weight of insulin (Lilly Humalog). Plasma was collected prior to intraperitoneal glucose injection for the assessment of plasma insulin. Insulin levels were measured via ELISA (Crystal Chem #90080). Glucose uptake was measured as previously reported [25]. Briefly, 5 μ Ci [14C]-2DG was infused intravenously, immediately before an intraperitoneal glucose injection (2.5 g/kg). Thirty minutes after the injection, mice were sacrificed, and tissues were snap-frozen in liquid N₂. Sample tissues were lysed in 1 N NaOH at 80 °C, followed by neutralization (~pH 7.5) with 12 N HCl. Supernatants were extracted with Ba(OH)₂-ZnSO₄ (i.e., Somogyi method [26]). Reported 2-deoxyglucose phosphate was defined as the difference between the radioactivity of the neutralized and extracted supernatant. BAT tissue was harvested for insulin signaling 10 min after an intraperitoneal injection of 1 U/kg body weight of insulin. Core body temperature was assessed hourly during a 4 h cold challenge using a rodent rectal probe (Microtherma 2, Thermoworks). After collecting basal core body temperature at 28 °C, mice were individually separated into empty boxes without food, water, or bedding, then placed at 4 °C.

2.8. Histology

The gross morphology of BAT tissue was imaged with a 16 MP camera. BAT was fixed for 6 h in 4% paraformaldehyde diluted in PBS at 4 °C, then embedded in paraffin for the histological analysis. Sections were cut at 6 μ m for hematoxylin and eosin (H&E) staining. Slides were imaged using an Olympus IX81 fluorescence microscope and processed using the count and measure feature on CellSens Dimension software version 1.12 (Olympus). Lipid droplet size was quantified from male mice (n = 3–4) using CellSens Dimension version 1.12 software from duplicate or triplicate slides.

2.9. Quantitative real-time PCR

RNA was isolated from cultured cells or the whole tissue using the RNeasy Lipid Mini Kit (Qiagen; #74136) according to the manufacturer's instructions. Complementary DNA was synthesized by RT-PCR using a Bio-Rad SuperScript III. Single-gene quantitative PCR was performed with iTaq SYBR Green (Bio-Rad; #172-5124) using a LightCycler 480 II (Roche Applied Science) or a CFX96 Real-Time System (Bio-Rad). Data were analyzed using the 2^{- $\Delta\Delta$ CT} method and normalized to the housekeeping gene *TATA-Box Binding Protein* (*TBP*, for mice), *ACTIN* (human), or *gapdh* (cell line). See Supplemental Tables 1 and 2 for primer sequences.

2.10. Chromatin Immunoprecipitation (ChIP)

BAT from C57Bl/6 mice was dissected, minced, fixed with 1% formaldehyde diluted in PBS for 20 min at room temperature, quenched

with 125 mM glycine for 5 min at room temperature, then homogenized using a tissue homogenizer (PowerGen 125; Fisher Scientific). Samples were then centrifuged at 4000 \times g for 5 min at 4 °C, the middle formaldehyde/PBS layer was removed and washed three times with PBS. Lysis buffer containing 1% SDS, 10 mM EDTA, and 50 mM Tris pH8 was added, and protein-DNA fragments were sonicated to a mean size of ~500 bp four times using 5 min intervals with 30 s on/off (Misonix Sonicator 3000). Sonicated samples were centrifuged at 10,000 \times g for 5 min at 4 °C, and the supernatant was collected. Chromatin was then incubated overnight at 4 °C with α -LDB1 (Santa Cruz; #sc-11198x) or control goat immunoglobulin G (Bethyl; Cat. P50-100). Chromatin complexes were precipitated with Protein G Dynabeads (Invitrogen by Thermo Fisher, #10003D) at 4 °C for 4 h, washed with a series of high salt, low salt, LiCl and TE buffer solutions, and eluted with an elution buffer consisting of 0.1 M NaHCO₃, 0.2% SDS, 5 M NaCl, and Proteinase K, and then crosslinks were reversed. Quantitative PCR was performed on the ChIP DNA using an SYBR Green PCR master mix (Bio-Rad). Enriched ChIP DNA was normalized to *Albumin* promoter DNA enrichment and calculated relative to IgG, set as one-fold ($\Delta\Delta$ CT) [11,20,24]. ChIP experiments were performed with independent chromatin preparations. Primers were designed to flank putative A/T-rich homeodomain binding elements (i.e., core TAAT/ATTA) in the *Ucp1* proximal promoter and distal enhancer region. See Supplemental Table 2 for primer sequences.

2.11. Statistical analysis

All data are represented as mean \pm standard error of the mean (SEM). Statistical significance was calculated using either unpaired Student's *t*-tests or one- and two-way analysis of variance (ANOVA), where appropriate. This analysis was followed by multiple-comparison Tukey and Sidak post-tests, respectively. All statistical measures were completed using GraphPad Prism version 8.0 (GraphPad Software). Statistical significance was assigned at *P* < 0.05.

3. RESULTS

3.1. LDB1 is required for the expression of thermogenic BAT genes *in vitro*

We assessed two *in vitro* models of *Ldb1* deficiency to examine the LDB1 effects on brown adipocyte gene expression. We first conducted an *siLdb1* knockdown in the UCP1+ X9 adipocyte cell line (20). After differentiation, an *Ldb1*-specific siRNA transfection resulted in significant *Ldb1* mRNA reduction, compared to scramble (SiScr) controls (Figure 1A). We employed a β 3-AR agonist CL-316,243 (CL) to induce thermogenic gene expression and *Ucp1* transcription compared to the DMSO vehicle (V). There was no difference in *Ucp1* mRNA in *siLdb1* cells treated with CL or V (Figure 1B), suggesting LDB1 is required for *Ucp1* induction upon agonist treatment. We next transduced cultured primary brown adipocytes isolated from *Ldb1*^{Flox} mice with either an adenovirus expressing Cre recombinase to elicit *Ldb1* recombination or a LacZ control. Transduced cells were cultured in differentiation media then CL-treated before harvesting (Figure 1C). Cre-transduced adipocytes had reduced *Ldb1* and *Ucp1* protein and mRNA compared to LacZ controls (Figure 1D–F). LacZ and Cre-transduced adipocytes were treated with a CL agonist to evaluate impacts on *Ucp1* induction. CL-treatment in control cells (LacZ + CL) significantly induced *Ucp1* mRNA (Figure 1F). However, *Ldb1*-deficient adipocytes treated with the agonist (Cre + CL) had impaired *Ucp1* induction, both relative to LacZ control and the fold induction to Cre + Vehicle control (Figure 1F). Next, we assessed whether LDB1 effects are specific to brown adipocytes or general adipocyte differentiation *in vitro* independent of CL

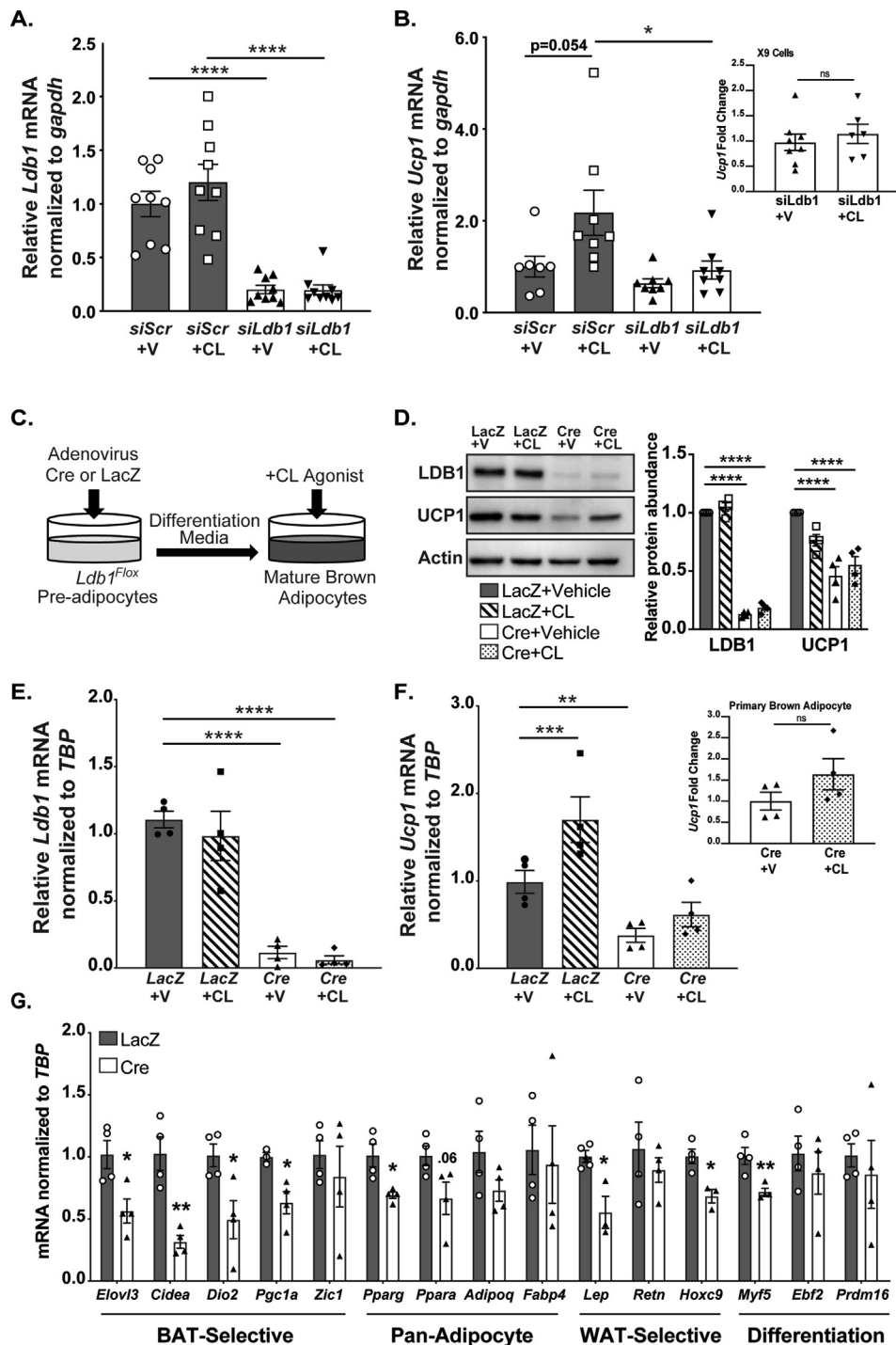


Figure 1: LDB1 is required for the expression of thermogenic BAT genes *in vitro*. (A–B) *Ldb1* and *Ucp1* mRNA quantification from *siLdb1* or control siScramble (*siScr*) transfected and vehicle (V) or agonist (CL) treated X9 cells reveals that knockdown of *Ldb1* results in significantly reduced *Ucp1* mRNA in agonist treated cells (n = 7–9). Right, inset of *Ucp1* fold change in X9 cells comparing *siLdb1* knockdown with vehicle (V) and CL agonist treatment. (C) Schematic showing experimental design of *Ldb1* recombination in primary cell culture. (D) Western blot assessing LDB1 and UCP1 protein levels as compared to Actin loading control upon LacZ- or Cre-expressing adenoviral transduction and agonist (CL) or DMSO vehicle treatment of primary *Ldb1^{Flox}* cells (n = 4); Right panel is the quantification of western blots via densitometry of LDB1 and UCP1 protein band intensity normalized to Actin. (E–F) *Ldb1* and *Ucp1* mRNA quantification upon LacZ- or Cre-expressing adenoviral transduction and agonist (CL) or vehicle treatment of primary *Ldb1^{Flox}* cells (n = 4). Right, inset of *Ucp1* fold change of Cre-expressing adenoviral transduced primary brown adipocytes treated with vehicle (V) or CL agonist. ns, not significant via Student's *t*-tests. (G) qRT-PCR analyses of adipocyte and differentiation markers in Adeno-LacZ or Cre-treated cells (n = 3–4); *p < 0.05, **p < 0.01, ***p < 0.001, ****p < 0.0001 via Student's *t*-tests or one- and two-way ANOVA, where appropriate.

treatment. *Ldb1*-deficient cells had significant reductions in brown adipocyte markers *Elovl3*, *Cidea*, *Pgc1a*, and *Dio2* (Figure 1G). We also observed reductions of pan-adipocyte markers *Pparg* and *Ppara*, WAT-selective markers *Lep* and *Hoxc9* and the *Myf5* progenitor differentiation marker (Figure 1G). Additionally, we found mRNA involved in lipid uptake (e.g., *Lpl* and *Cd36*) and fatty acid oxidation, including *Acadl*, *Acadm*, and *Cpt1b*, reduced upon *Ldb1* loss (Sup Fig. 1). This finding suggests that without CL induction, LDB1 may be required for the expression of brown selective markers related to adipocyte differentiation and basal function *in vitro*. However, not all markers related to

adipocyte maturation and differentiation were reduced (Figure 1G, Sup Fig. 1), highlighting the specificity of LDB1 effects on brown adipocyte genes, rather than a general loss of transcription.

3.2. Expression of thermogenic related mRNA requires LDB1 *in vivo*

We employed a conditional knockout strategy via the recombination of an *Ldb1*^{Flox} allele driven by *Ucp1*-Cre, termed *Ldb1*^{ΔBAT} (Figure 2A), to directly test the role of LDB1 in regulating BAT function *in vivo*. An assessment of body weight over time showed no difference between

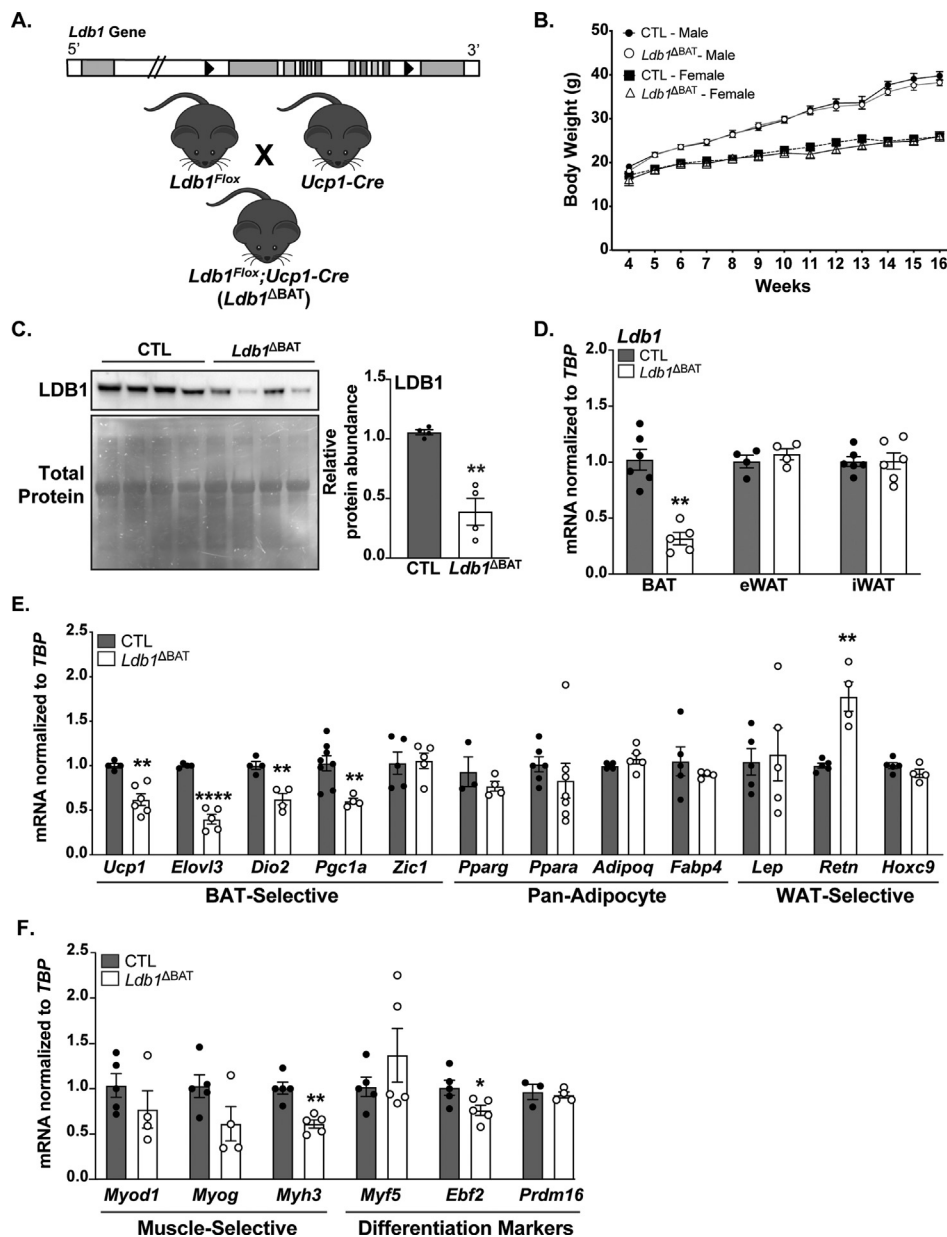


Figure 2: Expression of thermogenic related mRNA requires LDB1 *in vivo*. (A) Schematic of the *Ldb1* locus with approximate location of LoxP sites and breeding scheme to generate the *Ldb1*^{ΔBAT} mouse model. LoxP sites, approximately 3 kb apart, are represented by black triangles, and *Ldb1* exons are gray rectangles. (B) *Ldb1*^{ΔBAT} and control (CTL) male and female mouse body weights (n = 12–18). (C) Western blot assessing protein levels of LDB1 in male *Ldb1*^{ΔBAT} and CTL littermates (n = 4). Right panel is the quantification of western blots by densitometry of LDB1 protein band intensity compared to total protein. (D) Assessment of *Ldb1* mRNA from BAT, epididymal white adipose (eWAT), and inguinal white adipose (iWAT) tissue extracted from male mice (n = 4–6). (E–F) qRT-PCR analyses of brown adipocyte, pan-adipocyte, white adipocyte, muscle, and progenitor differentiation markers from BAT isolated from male *Ldb1*^{ΔBAT} and CTL littermates (n = 3–7). *p < 0.05, **p < 0.01; ****p < 0.0001; ns, not significant via Student's *t*-tests.

Ldb1^{ΔBAT} and CTL mice for both sexes (Figure 2B). For the characterization of this model, all mice were housed long-term at 28 °C, near thermoneutrality [17]. As BAT is the primary adipose depot expressing *Ucp1* at this temperature, a cold-induced Cre expression in other adipose depots should be limited [16]. Mature adipocytes were isolated from CTL and *Ldb1*^{ΔBAT} mice to assess the efficiency of LDB1 loss. Compared to CTL, *Ldb1* mRNA and protein were significantly reduced by >60% in *Ldb1*^{ΔBAT} mice (Figure 2C–D, Sup Fig. 2). This moderate but not complete loss could be due to the relatively large distance between LoxP sites (approximately 3 kb) within the *Ldb1* locus or incomplete penetrance of the Cre transgene. In addition, without sorting *Ldb1*-deficient mature brown adipocytes, we could not reveal potentially greater recombination efficiency in purified Cre⁺ cells. *Ldb1* mRNA levels were compared between BAT, epididymal, and inguinal white adipocyte depots from CTL and *Ldb1*^{ΔBAT} male mice to determine the tissue specificity of the recombination. *Ldb1* reductions were restricted to brown adipocytes (Figure 2D). Even with a 60% loss of LDB1 in BAT (Figure 2C–D), mRNA-encoding BAT-selective thermogenic regulators, including *Ucp1*, *Elovl3*, *Dio2*, and *Pgc1a*, were reduced, whereas the brown adipocyte marker *Zic1* was unchanged (Figure 2E). This finding corroborates the *in vitro* results above (Figure 1) and our previous *Ldb1*^{+/-} study. Markers for adipogenesis, myogenesis, and differentiation were evaluated to determine if the reductions in specific thermogenic mRNA were due to altered adipocyte differentiation. Adipogenic markers *Pparg* and *Ppara* (both of which encode two transcriptional regulators of adipocyte function) and *Adipoq* and *Fabp4* (both of which are involved in lipid metabolism in mature adipocytes) were unchanged in *Ldb1*^{ΔBAT} mice (Figure 2E). White adipocyte selective markers *Lep* and *Hoxc9* were also unchanged, whereas *Retn* was increased in *Ldb1*^{ΔBAT} mice. Myogenic regulatory factors *Myog* and *Myod1* were unaffected, whereas the muscle-associated structural gene *Myh3* was reduced (Figure 2F). Transcriptional regulators *Myf5* and *Prdm16*, both associated with progenitor differentiation, were unchanged, whereas *Ebf2*, a late marker of brown adipocyte maturation, was slightly reduced (Figure 2F). Overall, these data suggest that LDB1 is necessary for the maintenance of the thermogenic identity of mature brown adipocytes.

3.3. LDB1 occupies upstream *Ucp1* regulatory domains, has several potential BAT-expressed partners, and is enriched in human supraclavicular adipose

Having observed the impacts of LDB1 on *Ucp1* expression, we hypothesized that LDB1 might occupy *Ucp1* regulatory regions to control thermogenic gene expression. We examined whether LDB1 occupies the previously described *Ucp1* promoter and/or enhancer regions [27]. As LDB1 lacks DNA-binding capacity, we designed ChIP primers flanking one A/T-rich putative LIM-homeodomain (HD) binding element within the *Ucp1* proximal promoter and two within the enhancer (Figure 3A). With chromatin from either induced immortalized brown adipocytes [22] or primary BAT, we observed significant LDB1 enrichment in the *Ucp1* enhancer, spanning HD elements 2 or 3, and within the proximal promoter spanning HD element 1, compared to IgG control (Figure 3B–C). Given that LDB1 forms large transcriptional complexes, we next wanted to assess potential LIM-factor interacting partners required to elicit LDB1 function. A LIM-factor survey in BAT revealed an enrichment of LIM-only factors (LMO), *Lmo2* and *Lmo4*, in addition to *Lhx8* (Figure 3D). An assessment of BAT extracted at 28 °C, and 4 °C revealed *Ldb1*, *Lhx8*, and *Lmo2* mRNA levels were reduced in response to cold, whereas *Lmo4* remained unchanged (Figure 3E). Compared to preadipocytes in the SVF fraction, *Ucp1*, *Ldb1*, and *Lmo4*

were enriched, *Lhx8* was decreased, and *Lmo2* remained unchanged in mature brown adipocytes (Figure 3F). Elevations of LDB1 and UCP1 protein upon differentiation were also observed in immortalized brown preadipocytes (Figure 3G). This finding supports a possible role for LDB1 in mature brown adipocytes and UCP1 induction. Overall, the varying expression of these factors suggests that LDB1 may interact with different LIM factor partners in a context-dependent manner. An assessment of human adipose biopsies revealed an overt enrichment of *LDB1* mRNA in supraclavicular adipose compared to subcutaneous white adipose (Figure 3H). The supraclavicular adipose, mostly comprised of brown adipocytes [4,5,28–30], also revealed an expected enrichment of *UCP1* and *LHX8*, known brown adipocyte markers in humans and mice [31–33], but lack of *Leptin*, a white adipose marker (Figure 3H). The supraclavicular *LDB1* enrichment suggests analogous roles in human and mouse BAT function.

3.4. Glucose tolerance and uptake are reduced upon loss of LDB1, in part via altered insulin signaling

Given the known importance of glucose to brown adipocyte function, we hypothesized that LDB1 might regulate glucose utilization, altering whole-body glucose homeostasis. Though the fasting blood glucose was unchanged between genotypes (Figure 4A), an intraperitoneal glucose tolerance test (IPGTT) revealed impaired glucose tolerance in male *Ldb1*^{ΔBAT} mice (Figure 4B). Given that glucose intolerance was only observed in males, we further conducted an intraperitoneal insulin tolerance test (IPITT) in male *Ldb1*^{ΔBAT} mice. Under thermoneutral conditions, insulin tolerance was similar between CTL and *Ldb1*^{ΔBAT} mice (Figure 4C). However, when the IPITT was performed after a cold challenge or CL injection, *Ldb1*^{ΔBAT} mice exhibited reduced glucose clearance, suggesting that LDB1 affects insulin action in active BAT (Figure 4D–E). An assessment of 2DG uptake uncovered impaired BAT glucose uptake in *Ldb1*^{ΔBAT} male mice (Figure 4F). This effect was specific to BAT, as uptake in other metabolic tissues (including the gastroc and heart) were similar regardless of genotype. Additionally, there was no difference in fasting plasma insulin at thermoneutrality between *Ldb1*^{ΔBAT} and CTL mice (Figure 4G), which led us to assess changes in insulin signaling. The quantification of insulin-stimulated AKT phosphorylation revealed decreased pAKT^{Ser473}, with increased pERK1/2 in BAT of *Ldb1*^{ΔBAT} mice (Figure 4H–G), supporting that mildly impaired glucose tolerance in *Ldb1*^{ΔBAT} mice may be due, in part, to altered insulin signaling.

3.5. LDB1 impacts brown adipocyte morphology and lipid metabolism

Brown adipocytes utilize intracellular and circulating lipids to fuel thermogenesis and maintain tissue function. Based on our observations, we predicted that LDB1 might regulate brown adipocyte lipid utilization and storage. Despite no overt differences in gross BAT morphology between CTL and *Ldb1*^{ΔBAT} mice, BAT weight was significantly increased in female *Ldb1*^{ΔBAT} mice, with a trending increase in males (Figure 5A–B). An assessment of adipocyte morphology and lipid droplet size at thermoneutrality revealed a trend toward slightly larger adipocytes and lipid droplets between groups (Figure 5C–D). After an acute 3 h cold challenge, lipid droplets of *Ldb1*^{ΔBAT} brown adipocytes were significantly larger than CTL (Figure 5E–F). Except for the increased plasma TG levels in *Ldb1*^{ΔBAT} mice at thermoneutrality, an assessment of plasma TG, free fatty acids (FFA), and cholesterol levels during a cold challenge revealed no differences between groups (Sup Fig. 3). This finding suggests that impairments in lipid handling may be specific to BAT. We assessed changes in BAT mRNA involved in fatty acid uptake, synthesis, and

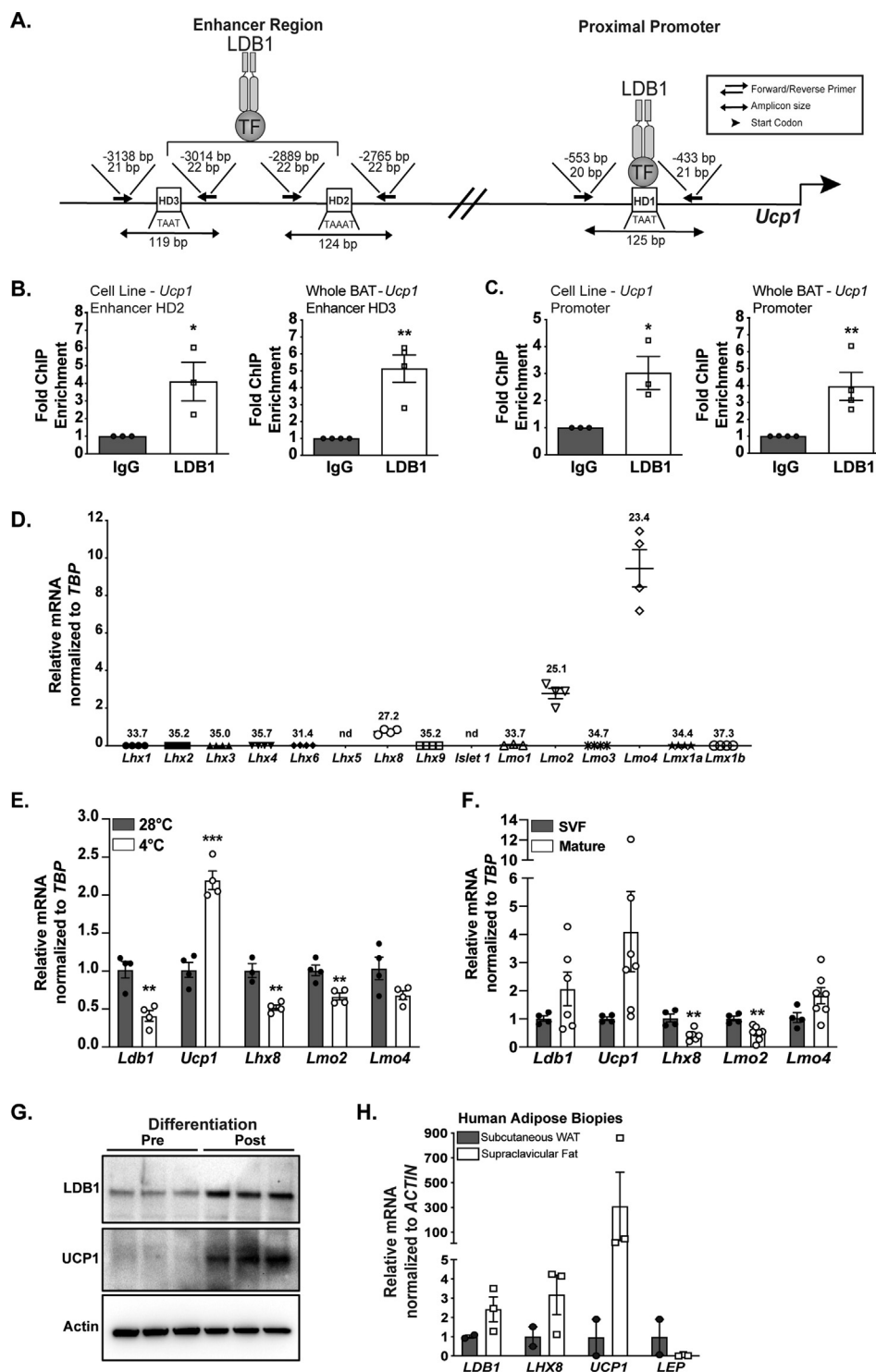


Figure 3: LDB1, which occupies the *Ucp1* regulatory domains and is enriched in human supraclavicular adipose, may partner with several BAT expressed LIM factors to regulate gene expression. (A) Schematic of putative homeodomain (HD) binding sites in the *Ucp1* promoter and enhancer region with primer locations and amplicon size denoted. (B–C) LDB1 ChIP of enhancer and promoter regions of *Ucp1* using chromatin isolated from a brown adipocyte cell line [22] (n = 3) or whole BAT (n = 4). (D) LIM factor survey assessing mRNA levels of LIM-HD and LMO transcriptional regulators relative to *TBP* in BAT (n = 4). Ct values for all mRNA tested are shown. (E) Comparison of mRNA markers using BAT from mice housed at 28 °C or after a 3-hour 4 °C cold challenge (n = 4). (F) Assessment of mRNA levels from SVF or mature adipocytes isolated from BAT of mice housed at 28 °C (n = 4–7). (G) Western blot showing protein expression of LDB1 and UCP1 before and after preadipocyte differentiation (n = 3). (H) Gene expression data from human adipose biopsies taken from subcutaneous WAT (black bar n = 2) and supraclavicular fat (i.e., thermogenic adipose, white bars n = 3). *p < 0.05; **p < 0.01; ***p < 0.001 via Student's *t*-tests.

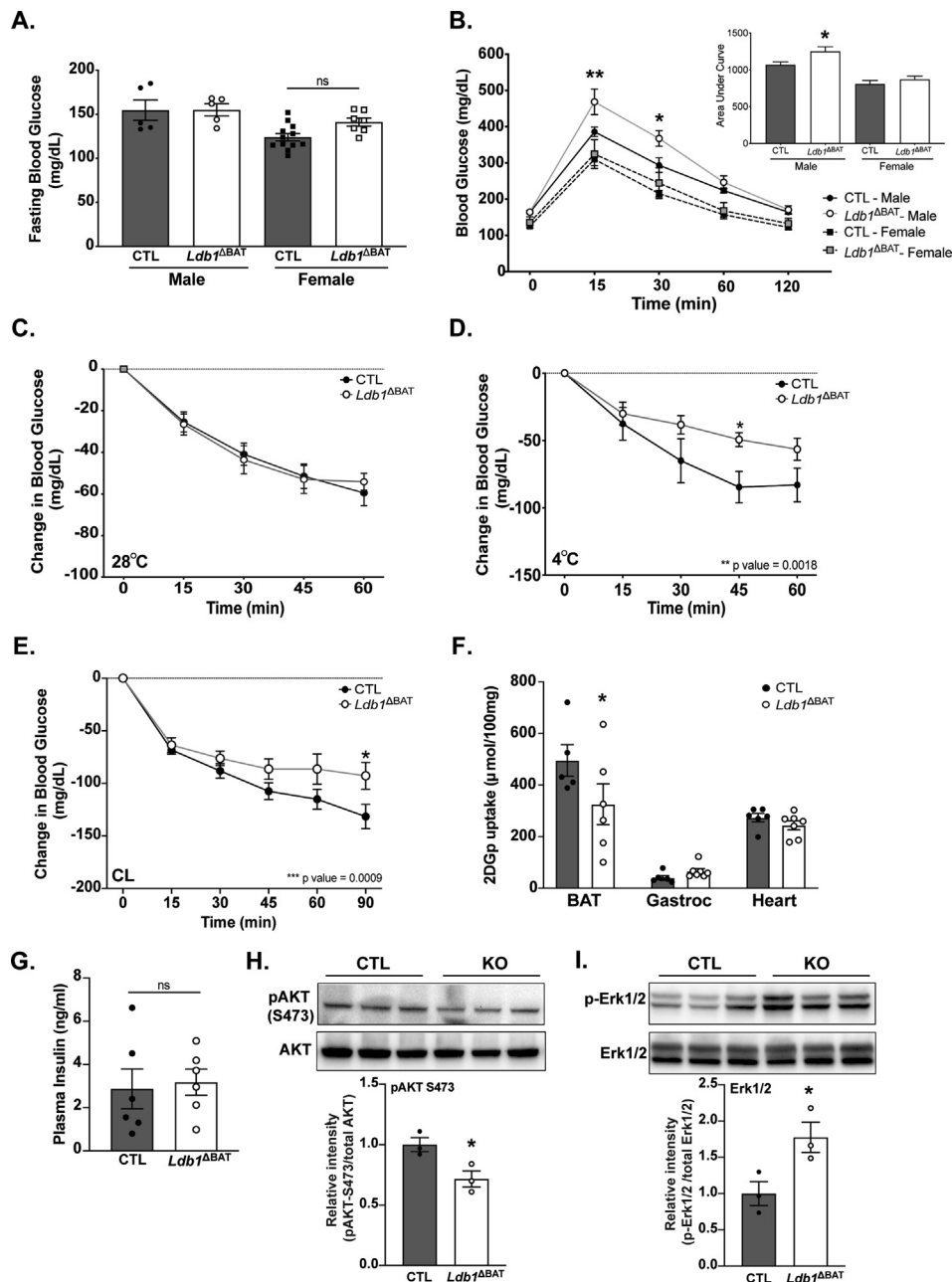


Figure 4: Glucose tolerance and uptake are reduced upon loss of LDB1, in part via altered insulin signaling. (A) Plasma blood glucose from male ($n = 5$) and female ($n = 11$) CTL and *Ldb1*^{ΔBAT} mice after a 6-h fast. (B) Intraperitoneal glucose tolerance tests (IPGTT) after injection of 2.0 g/kg body weight of glucose for CTL and *Ldb1*^{ΔBAT} mice raised at 28 °C for female mice (CTL $n = 11$ and *Ldb1*^{ΔBAT} $n = 12$) and male mice (CTL $n = 5$ and *Ldb1*^{ΔBAT} $n = 4$) aged 2–4 months. Inset shows Area Under the Curve (AUC). (C) Intraperitoneal insulin tolerance tests (IPITT) to assess changes in blood glucose upon injection of 0.5U/kg body weight of insulin in CTL and *Ldb1*^{ΔBAT} male mice at 28 °C ($n = 5–6$). (D–E) IPITT conducted in male mice 15 min after an acute 4 °C cold challenge or CL316,243 injection, respectively ($n = 5–6$; aged 3-month-old). Genotype effect found on lower right corner calculated via 2-way ANOVA. (F) Glucose uptake via 2DG glucose tracer in male mice ($n = 5–7$; 8–9-month-old). (G) Plasma insulin assessed via ELISA from CTL and *Ldb1*^{ΔBAT} male mice at 28 °C ($n = 6$). (H) Assessment via western for pan or pAKT^{S473} protein ($n = 3$); Bottom panel is densitometry of pAKT^{S473} protein band intensity normalized to pan AKT. (I) Assessment via western of total and p-Erk1/2 protein ($n = 3$); Bottom panel is densitometry of p-Erk1/2 protein band intensity normalized to total Erk1/2 protein. *, $p < 0.05$; **, $p < 0.01$; ***, $p < 0.001$; ns, not significant via Student's *t*-tests or two-way ANOVA, where appropriate.

oxidation to explore this effect further. Except for *Cd36*, which was significantly reduced in *Ldb1*^{ΔBAT} mice, most markers of fatty acid uptake, including *Lpl* and *Fatp1*, were unchanged. An assessment of mRNA associated with fatty acid synthesis (including *Fasn*) and oxidation (including *Aca1*, *Acadm*, *Cpt1a*, and *Cpt1b*) revealed

reductions in the *Ldb1*^{ΔBAT} mice compared to CTL. Additionally, several mRNA associated with mitochondrial respiration, including *Cox*, *Nduf*, *Cycc*, *Cox8b*, and *Cox7a*, were also reduced in the *Ldb1*^{ΔBAT} mice. Together these data suggest that LDB1 regulates pathways involved in fatty acid oxidation in brown adipocytes.

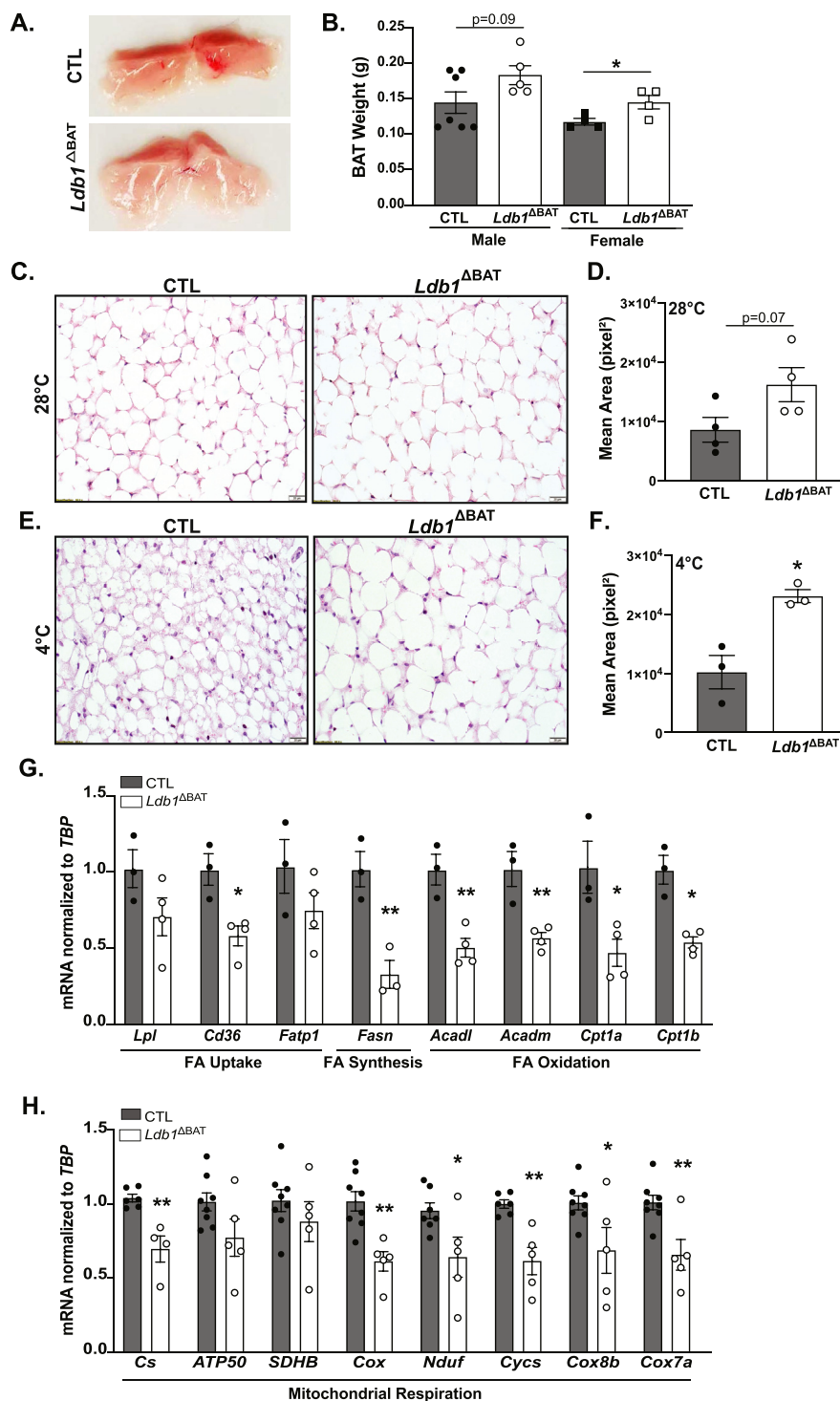


Figure 5: LDB1 impacts brown adipocyte morphology and lipid metabolism. (A) Gross morphology of BAT from *Ldb1*^{ΔBAT} and CTL male mice (n = 3). (B) BAT weight from male and female *Ldb1*^{ΔBAT} and CTL mice (n = 4–7). (C–F) BAT morphology assessed via H&E and lipid droplet size quantified as mean area (pixel²) from BAT extract at 28 °C (C–D) or after a 3-h 4 °C cold challenge (E–F) from male mice (n = 3–4). (G–H) qRT-PCR analyses of mRNA markers of fatty acid uptake, synthesis, and oxidation, as well as mitochondrial respiration (n = 3–8). *, p < 0.05; **p < 0.01; via Student's *t*-tests.

3.6. LDB1 is required for energy expenditure and thermogenic function

Having observed that LDB1 is required to maintain BAT gene expression and glucose/lipid homeostasis, we next examined whether LDB1 impacts BAT-driven EE and thermogenesis. EE was measured in

CTL and *Ldb1*^{ΔBAT} mice via indirect calorimetry at 26 °C, 24 °C, and 22 °C to assess if EE changes with temperature (Figure 6A–B). Both female and male cohorts followed a typical circadian EE pattern at all temperatures. For female mice, there was no EE difference observed between genotypes at 26 °C or 24 °C (Figure 6A). However, at 22 °C,

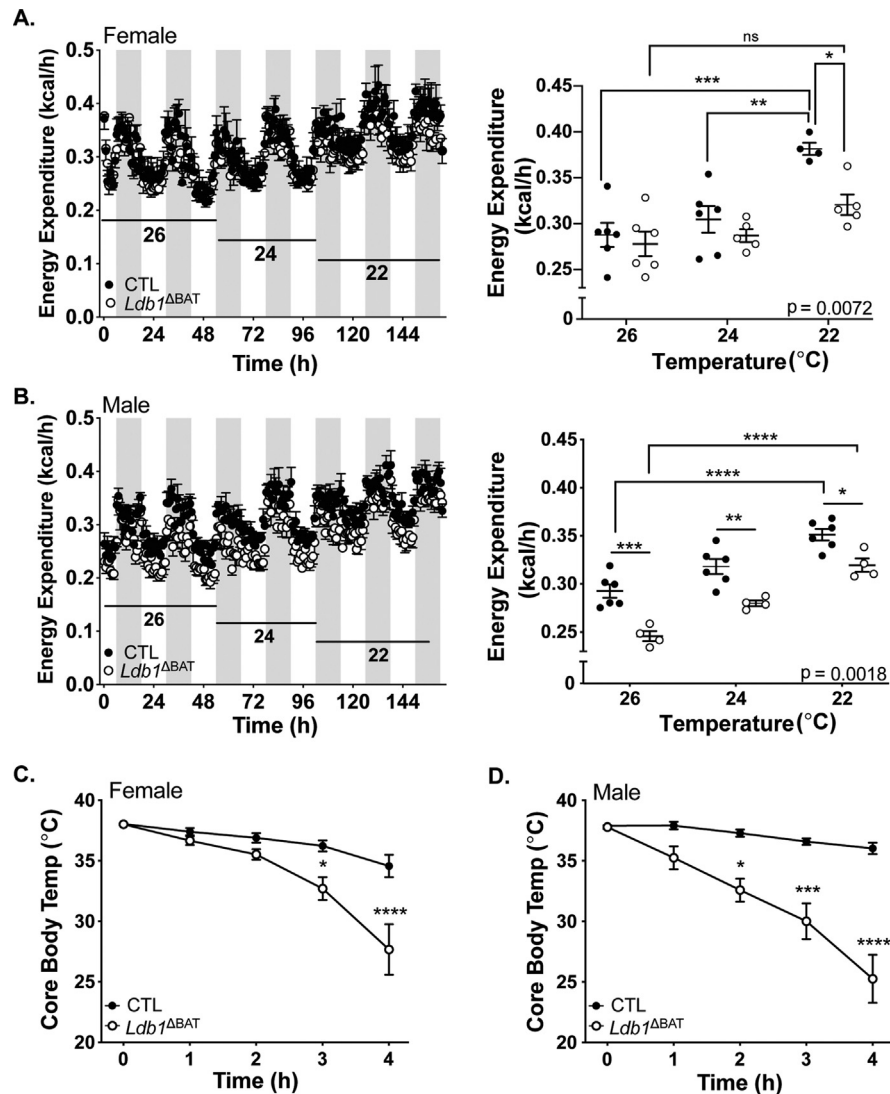


Figure 6: LDB1 is required for energy expenditure and thermogenic function. (A–B) Indirect calorimetry on female and male *Ldb1*^{ΔBAT} and CTL littermates. Energy expenditure (EE) was measured at three temperatures, 26 °C, 24 °C, and 22 °C, in chow-fed mice (n = 4–6), aged 5–6 months. Right panel is total EE quantified at 26 °C, 24 °C, and 22 °C. Genotype effect found on lower right corner calculated via 2-way ANOVA. (C–D) Four-hour cold challenge was conducted at 4 °C on (C) female mice (CTL n = 9 and *Ldb1*^{ΔBAT} n = 14) and (D) male mice (CTL n = 8 and *Ldb1*^{ΔBAT} n = 11) aged 2–4 months. *, p < 0.05; **, p < 0.01; ***, p < 0.001; ****, p < 0.0001; via Student's *t*-tests or two-way ANOVA, where appropriate.

when the thermogenic activity of BAT is higher, there was a significant reduction in EE in *Ldb1*^{ΔBAT} female mice compared to CTL (Figure 6A). Additionally, there was no temperature-dependent difference in EE in *Ldb1*^{ΔBAT} females, suggesting LDB1 is required for brown adipocyte activation (Figure 6A). Compared to CTL mice, EE was reduced at all temperatures in *Ldb1*^{ΔBAT} male mice (Figure 6B). These changes were independent of body composition, respiratory quotient, food intake, and locomotor activity, which were similar between genotypes (Sup Fig. 4). This finding suggests that BAT-expressed LDB1 is required for maintaining whole-body EE. Due to the EE impairments and observed reductions of BAT-selective mRNA, we hypothesized that BAT-mediated thermogenesis would be impaired upon LDB1 loss. We tested this hypothesis by conducting a 4 °C cold challenge with core body temperature measured at baseline (time = 0) and every hour thereafter, for up to 4 h. Strikingly, both female and male *Ldb1*^{ΔBAT} mice exhibited profound reductions in core body temperature over

time, compared to CTL mice (Figure 6C–D). These data strongly support that LDB1 regulates brown adipocyte-driven EE and thermogenesis.

4. DISCUSSION

Through complementary *in vitro* and *in vivo* deficiency models, we uncovered novel regulatory roles for LDB1 in brown adipocyte function. BAT-specific reductions of LDB1 resulted in impaired whole-body EE, cold intolerance, and altered lipid metabolism in male and female mice, as well as glucose intolerance in male mice. Cold intolerance in *Ldb1*^{ΔBAT} mice is consistent with other models of UCP1 deficiency, either through *Ucp1* knockout [7,8] or loss of *Ucp1* transcriptional regulators, including PRDM16 [10]. Though LDB1 may regulate *Ucp1* to affect cold tolerance, reductions in additional gene targets involved in lipid metabolism and thyroid signaling (e.g., *Elovl3*, *Dio2*) likely

contribute to the severe cold intolerance phenotype. Substrates like glucose and fatty acids are either oxidized as fuel for thermogenesis or used to replenish intercellular lipid pools [34,35]. Given the importance of metabolites for adipocyte thermogenesis, models affecting substrate uptake and utilization, including an adipose triglyceride lipase (ATGL) knockout model, also result in cold intolerance phenotypes [36]. *Ldb1*^{ΔBAT} male mice have impaired glucose uptake, whereas both male and female *Ldb1*^{ΔBAT} mice have apparent changes in fatty acid oxidation. Therefore, we hypothesized that the severe cold intolerance phenotype observed is due, in part, to changes in glucose and/or lipid metabolism. In support of this hypothesis, we found altered insulin signaling in male *Ldb1*^{ΔBAT} mice. Reductions in p-AKT^{S473}, a substrate of the IRS-1/PI3K/AKT pathway, may suggest LDB1 regulates pathways involved in insulin-induced lipid synthesis and *Ucp1* induction [37]. However, upon reductions in LDB1, we also found significant increases in p-Erk1/2, a substrate of the Grb-2/Ras/MAPK pathway, suggesting LDB1 may negatively regulate pathways involved in adipocyte proliferation [37]. This finding suggests that LDB1 can be both a positive and negative regulator of brown adipocyte function. Future studies will further elucidate brown adipocyte gene expression and cellular pathways, including those regulated by LDB1.

This study also revealed sex-dependent effects of BAT-expressed LDB1, consistent with prior studies characterizing BAT physiology. Previously, differences in BAT thermogenesis between sexes have been reported in rodents, with females showing a greater uncoupling capacity, higher mitochondrial content, and greater intracellular lipid content [38–41]. In humans, sex differences in energy metabolism and BAT activity have also been described, with females exhibiting lower EE and higher BAT activity than males [4,42,43]. In the *Ldb1*^{ΔBAT} model, we observed sex differences in both BAT EE and thermogenesis upon LDB1 loss. Compared to *Ldb1*^{ΔBAT} male mice, which had significant reductions in EE at all temperatures, female *Ldb1*^{ΔBAT} mice only displayed reduced EE at 22 °C. Additionally, a cold challenge revealed that male *Ldb1*^{ΔBAT} mice displayed the greatest reduction in core body temperature at 4 h. Sex differences in thermogenesis may be attributed to variations in basal uncoupling capacity, sympathetic activity, fat mass composition, and hormone signaling [41,44]. This difference also extends to metabolic parameters, like glucose and lipid homeostasis [45]. Previous studies highlighted differences in insulin sensitivity, insulin-stimulated glucose uptake, and lipogenesis in rodent adipocytes, with females being more resistant to metabolic dysregulation [46–48]. Additionally, genetic models utilizing HFD highlight the differential outcomes of sex on disease development [49,50]. For example, a model of *Id1* overexpression, a negative regulator of *Pgc1a* and brown adipose thermogenesis, showed that males but not females were susceptible to HFD-induced obesity. These sex differences are consistent with our model in which, despite reductions in *Ldb1* in both sexes, glucose homeostasis was maintained in females. Future studies will investigate the genes and signaling pathways differentially regulated in male and female *Ldb1*-deficient brown adipocytes in more depth.

As a transcriptional co-regulator, LDB1 directly interacts with LIM-homeodomain and LIM-only TF sub-classes to regulate gene targets [12,51]. The BAT LIM-factor survey revealed an enrichment of several LIM-factor mRNA, including *Lmo2*, *Lmo4*, and *Lhx8*. Though LHX8 is a known BAT marker (27–29), its role in brown adipose is largely unknown. Previously, *Lhx8* mRNA levels were shown to decrease in brown adipocytes in response to cold [52], as our findings confirm. In addition to LHX8, LMO proteins, including LMO2 and LMO4, are transcriptional adapters that affect gene expression through interactions within larger transcriptional complexes. In human visceral

adipocytes, LMO3 promotes adipocyte differentiation via the regulation of PPAR γ activity [53]. In mice, LMO4, the highest expressed factor in our LIM survey, was implicated in regulating preadipocyte proliferation and adipogenesis [54]. Though these data support a potential role for LDB1-LMO factor complexes in regulating BAT function, LIM-factor antibody limitations precluded us from assessing which LIM factor(s) mediate LDB1 action in BAT.

The range of interacting partners affords LDB1-containing complexes a broader potential to regulate brown adipocyte transcription. Through LMO adapters, LDB1 can also indirectly interact with basic helix-loop-helix (bHLH) and GATA TF classes to affect gene expression [12]. For example, GATA2, a potential LDB1 interacting partner, has been linked to brown adipocyte differentiation [55]. Additionally, we found LDB1 occupying *Ucp1* regulatory regions enriched by sequences of other critical BAT TFs and co-regulators, including PPAR γ , PGC1 α , and C/EBP [9,27]. Many of these transcriptional regulators participate in large multi-protein complexes, which regulate *Ucp1* expression. Examples include PRDM16 and PGC1 α co-regulators, which stabilize transcriptional complexes involving PPAR TFs [56]. The occupancy of LDB1 in the *Ucp1* enhancer and promoter regions may allow for potential interaction with these regulators. Future studies utilizing mass spectrometry may help to define BAT-specific LDB1-interacting partners. Throughout this study, various models of LDB1 loss highlighted the requirement of LDB1 for brown adipocyte function and gene expression. Reductions in thermogenic mRNA levels could be due to the loss of stability of LDB1-mediated multi-protein complexes. Given the detrimental effects observed upon reductions in LDB1, it is tempting to propose the over-expression of this co-regulator as a potential mechanism to improve BAT function. However, genetic models employing the over-expression of LDB1 or interacting LIM-HD TF interactors alone have resulted in dominant negative effects on cellular processes [57–59]. The misexpression of LDB1 or LMO2 resulted in the inhibition of erythroid differentiation [57,60]. Additionally, the over-expression of the *Drosophila* ortholog of LDB1 (known as Chip) resulted in similar wing formation defects in knockout mutants, likely due to disruptions in protein complex stoichiometry [61]. These single-gene over-expression defects were rescued upon the co-expression of LDB1 and the *Drosophila* ortholog of Lhx2 (known as apterous), thus restoring the stoichiometry of the complex. This LIM stoichiometry consists of a tetramer of two dimerized LDB1 proteins bound directly by two LIM-factors to achieve proper function [12]. Negative impacts conferred by both gain- and loss-of-function models highlight the role of LDB1 stoichiometry in maintaining the integrity of multi-protein complexes and, therefore, normal cellular processes [57,62]. Given that LDB1 is required to maintain brown adipocyte function, identifying factors that *trans*-activate *Ldb1* expression would allow for more specific therapeutic targeting of LDB1-containing complexes. However, there are no known regulators of the *Ldb1* gene described in brown adipocytes.

Establishing LDB1 in brown adipose thermogenesis and substrate utilization serves as an entry point for the future assessment of this co-regulator in other cellular processes. Given reductions in several mRNAs involved in adipocyte differentiation in primary brown adipocytes (Figure 1), utilizing an *Myf5*-Cre mouse model may further clarify the role of LDB1 in preadipocyte differentiation. Additionally, models utilizing a high-fat diet may provide a greater understanding of LDB1 regulation under conditions of metabolic dysregulation. The apparent enrichment of *LDB1* and the putative partner *LHX8* in human BAT supports the supposition that LDB1 may have conserved roles across species. The identification of LIM-factor regulators acting in BAT or the development of small molecules that can stabilize LDB1-containing

complexes may enhance the therapeutic potential of LDB1 for the treatment of metabolic diseases.

AUTHOR CONTRIBUTIONS

JDK and CSH directed the study. JDK and CSH wrote and edited the manuscript. *In vitro* studies were completed by JDK, TK, and YL. GR provided reagents and guidance on experimental design for adenoviral transfection. *In vivo* experiments were conducted by JDK. Indirect calorimetry was conducted by MY, with analysis performed by JDK and KMH. Analysis of human adipose tissue was conducted by CC, JWJ, and AMC.

ACKNOWLEDGMENTS

Funding support: The authors were supported by the NIH: R01DK111483 (to CSH), F31DK121414 and T32GM109780 (to JDK), 1R01DK112934 and P30DK079626 (to KMH), the Intramural Research Program of the NIDDK: DK075112 and DK075115 (to AMC).

Assistance: We thank Maigen Bethea, Eliana Toren, and Tanya Pierre (University of Alabama at Birmingham) for manuscript comments. We thank David Kleiner, Mohammed Mahbood, Sarah Young, Willie Young, and the Laboratory of Pathology at the NIH Clinical Center. We also thank Dr. Kai Ge at the NIH-NIDDK for providing the immortalized preadipocytes for ChIP studies and Dr. Paul Love at the NIH-NICHD for sharing the rabbit anti-LDB1 antibody. The University of Alabama at Birmingham Small Animal Phenotyping Core used in these studies was supported by the National Institute of Diabetes and Digestive and Kidney Diseases Grant P30 DK056336. The content of this work is solely the responsibility of the authors and does not necessarily represent the official views of the National Institutes of Health.

CONFLICT OF INTEREST

The authors have declared that no conflict of interest exists.

APPENDIX A. SUPPLEMENTARY DATA

Supplementary data to this article can be found online at <https://doi.org/10.1016/j.molmet.2021.101284>.

REFERENCES

- [1] Bartelt, A., Bruns, O.T., Reimer, R., Hohenberg, H., Itrich, H., Peldschus, K., et al., 2011. Brown adipose tissue activity controls triglyceride clearance. *Nature Medicine* 17(2):200–205.
- [2] Nedergaard, J., Bengtsson, T., Cannon, B., 2011. New powers of brown fat: fighting the metabolic syndrome. *Cell Metabolism* 13(3):238–240.
- [3] Stanford, K.I., Middelbeek, R.J., Townsend, K.L., An, D., Nygaard, E.B., Hitchcox, K.M., et al., 2013. Brown adipose tissue regulates glucose homeostasis and insulin sensitivity. *Journal of Clinical Investigation* 123(1):215–223.
- [4] Cypess, A.M., Lehman, S., Williams, G., Tal, I., Rodman, D., Goldfine, A.B., et al., 2009. Identification and importance of brown adipose tissue in adult humans. *New England Journal of Medicine* 360(15):1509–1517.
- [5] van Marken Lichtenbelt, W.D., Vanhomerig, J.W., Smulders, N.M., Drossaerts, J.M., Kemerink, G.J., Bouvy, N.D., et al., 2009. Cold-activated brown adipose tissue in healthy men. *N Engl J Med* 360(15):1500–1508.
- [6] Fedorenko, A., Lishko, P.V., Kirichok, Y., 2012. Mechanism of fatty-acid-dependent UCP1 uncoupling in brown fat mitochondria. *Cell* 151(2):400–413.
- [7] Enerback, S., Jacobsson, A., Simpson, E.M., Guerra, C., Yamashita, H., Harper, M.E., et al., 1997. Mice lacking mitochondrial uncoupling protein are cold-sensitive but not obese. *Nature* 387(6628):90–94.
- [8] Ukropec, J., Anunciado, R.V., Ravussin, Y., Kozak, L.P., 2006. Leptin is required for uncoupling protein-1-independent thermogenesis during cold stress. *Endocrinology* 147(5):2468–2480.
- [9] Collins, S., Yehuda-Shnaidman, E., Wang, H., 2010. Positive and negative control of Ucp1 gene transcription and the role of beta-adrenergic signaling networks. *International Journal of Obesity (Lond)* 34(Suppl 1):S28–S33.
- [10] Harms, M.J., Ishibashi, J., Wang, W., Lim, H.W., Goyama, S., Sato, T., et al., 2014. Prdm16 is required for the maintenance of brown adipocyte identity and function in adult mice. *Cell Metabolism* 19(4):593–604.
- [11] Loyd, C., Liu, Y., Kim, T., Holleman, C., Galloway, J., Bethea, M., et al., 2017. LDB1 regulates energy homeostasis during diet-induced obesity. *Endocrinology* 158(5):1289–1297.
- [12] Matthews, J.M., Visvader, J.E., 2003. LIM-domain-binding protein 1: a multifunctional cofactor that interacts with diverse proteins. *EMBO Reports* 4(12):1132–1137.
- [13] Hunter, C.S., Dixit, S., Cohen, T., Ediger, B., Wilcox, C., Ferreira, M., et al., 2013. Islet alpha-, beta-, and delta-cell development is controlled by the Ldb1 coregulator, acting primarily with the islet-1 transcription factor. *Diabetes* 62(3):875–886.
- [14] Zhao, Y., Kwan, K.M., Mailloux, C.M., Lee, W.K., Grinberg, A., Wurst, W., et al., 2007. LIM-homeodomain proteins Lhx1 and Lhx5, and their cofactor Ldb1, control Purkinje cell differentiation in the developing cerebellum. *Proceedings of the National Academy of Sciences of the U S A* 104(32):13182–13186.
- [15] Agulnick, A.D., Taira, M., Breen, J.J., Tanaka, T., Dawid, I.B., Westphal, H., 1996. Interactions of the LIM-domain-binding factor Ldb1 with LIM homeodomain proteins. *Nature* 384(6606):270–272.
- [16] Kong, X., Banks, A., Liu, T., Kazak, L., Rao, R.R., Cohen, P., et al., 2014. IRF4 is a key thermogenic transcriptional partner of PGC-1alpha. *Cell* 158(1):69–83.
- [17] Skop, V., Guo, J., Liu, N., Xiao, C., Hall, K.D., Gavrilova, O., et al., 2020. Mouse thermoregulation: introducing the concept of the thermoneutral point. *Cell Reports* 31(2):107501.
- [18] Fasshauer, M., Klein, J., Ueki, K., Kriauciunas, K.M., Benito, M., White, M.F., et al., 2000. Essential role of insulin receptor substrate-2 in insulin stimulation of Glut4 translocation and glucose uptake in brown adipocytes. *Journal of Biological Chemistry* 275(33):25494–25501.
- [19] de Souza, C.J., Hirshman, M.F., Horton, E.S., 1997. CL-316,243, a beta3-specific adrenoceptor agonist, enhances insulin-stimulated glucose disposal in nonobese rats. *Diabetes* 46(8):1257–1263.
- [20] Bethea, M., Liu, Y., Wade, A.K., Mullen, R., Gupta, R., Gelfanov, V., et al., 2019. The islet-expressed Lhx1 transcription factor interacts with Islet-1 and contributes to glucose homeostasis. *American Journal of Physiology. Endocrinology and Metabolism* 316(3):E397–E409.
- [21] Wu, J., Bostrom, P., Sparks, L.M., Ye, L., Choi, J.H., Giang, A.H., et al., 2012. Beige adipocytes are a distinct type of thermogenic fat cell in mouse and human. *Cell* 150(2):366–376.
- [22] Lai, B., Lee, J.E., Jang, Y., Wang, L., Peng, W., Ge, K., 2017. MLL3/MLL4 are required for CBP/p300 binding on enhancers and super-enhancer formation in brown adipogenesis. *Nucleic Acids Research* 45(11):6388–6403.
- [23] Habegger, K.M., Stemmer, K., Cheng, C., Muller, T.D., Heppner, K.M., Ottaway, N., et al., 2013. Fibroblast growth factor 21 mediates specific glucagon actions. *Diabetes* 62(5):1453–1463.
- [24] Wade, A.K., Liu, Y., Bethea, M.M., Toren, E., Tse, H.M., Hunter, C.S., 2019. LIM-domain transcription complexes interact with ring-finger ubiquitin ligases and thereby impact islet beta-cell function. *Journal of Biological Chemistry* 294(31):11728–11740.
- [25] Kim, T., Holleman, C.L., Nason, S., Arble, D.M., Ottaway, N., Chabenne, J., et al., 2018. Hepatic glucagon receptor signaling enhances insulin-stimulated glucose disposal in rodents. *Diabetes* 67(11):2157–2166.
- [26] Somogyi, M., 1945. Determination of blood sugar. *Journal of Biological Chemistry* 160(1):69–73.

- [27] Villarroya, F., Peyrou, M., Giralt, M., 2017. Transcriptional regulation of the uncoupling protein-1 gene. *Biochimie* 134:86–92.
- [28] van Marken Lichtenbelt, W.D., Vanhommerig, J.W., Smulders, N.M., Drossaerts, J.M., Kemerink, G.J., Bouvy, N.D., et al., 2009. Cold-activated brown adipose tissue in healthy men. *New England Journal of Medicine* 360(15):1500–1508.
- [29] Nedergaard, J., Bengtsson, T., Cannon, B., 2007. Unexpected evidence for active brown adipose tissue in adult humans. *American Journal of Physiology. Endocrinology and Metabolism* 293(2):E444–E452.
- [30] Saito, M., Okamatsu-Ogura, Y., Matsushita, M., Watanabe, K., Yoneshiro, T., Nio-Kobayashi, J., et al., 2009. High incidence of metabolically active brown adipose tissue in healthy adult humans: effects of cold exposure and adiposity. *Diabetes* 58(7):1526–1531.
- [31] Seale, P., Kajimura, S., Yang, W., Chin, S., Rohas, L.M., Uldry, M., et al., 2007. Transcriptional control of brown fat determination by PRDM16. *Cell Metabolism* 6(1):38–54.
- [32] Timmons, J.A., Wennmalm, K., Larsson, O., Walden, T.B., Lassmann, T., Petrovic, N., et al., 2007. Myogenic gene expression signature establishes that brown and white adipocytes originate from distinct cell lineages. *Proceedings of the National Academy of Sciences of the U S A* 104(11):4401–4406.
- [33] Sharp, L.Z., Shinoda, K., Ohno, H., Scheel, D.W., Tomoda, E., Ruiz, L., et al., 2012. Human BAT possesses molecular signatures that resemble beige/brite cells. *PLoS One* 7(11):e49452.
- [34] McNeill, B.T., Morton, N.M., Stimson, R.H., 2020. Substrate utilization by Brown adipose tissue: what's hot and what's not? *Frontiers in Endocrinology* 11:571659.
- [35] Labbe, S.M., Caron, A., Bakan, I., Laplante, M., Carpentier, A.C., Lecomte, R., et al., 2015. In vivo measurement of energy substrate contribution to cold-induced brown adipose tissue thermogenesis. *The FASEB Journal* 29(5):2046–2058.
- [36] Haemmerle, G., Lass, A., Zimmermann, R., Gorkiewicz, G., Meyer, C., Rozman, J., et al., 2006. Defective lipolysis and altered energy metabolism in mice lacking adipose triglyceride lipase. *Science* 312(5774):734–737.
- [37] Valverde, A.M., Benito, M., Lorenzo, M., 2005. The brown adipose cell: a model for understanding the molecular mechanisms of insulin resistance. *Acta Physiologica Scandinavica* 183(1):59–73.
- [38] Roca, P., Rodriguez, A.M., Oliver, P., Bonet, M.L., Quevedo, S., Pico, C., et al., 1999. Brown adipose tissue response to cafeteria diet-feeding involves induction of the UCP2 gene and is impaired in female rats as compared to males. *Pflügers Archiv* 438(5):628–634.
- [39] Quevedo, S., Roca, P., Pico, C., Palou, A., 1998. Sex-associated differences in cold-induced UCP1 synthesis in rodent brown adipose tissue. *Pflügers Archiv* 436(5):689–695.
- [40] Valle, A., Garcia-Palmer, F.J., Oliver, J., Roca, P., 2007. Sex differences in brown adipose tissue thermogenic features during caloric restriction. *Cellular Physiology and Biochemistry* 19(1–4):195–204.
- [41] Rodriguez-Cuenca, S., Pujol, E., Justo, R., Frontera, M., Oliver, J., Gianotti, M., et al., 2002. Sex-dependent thermogenesis, differences in mitochondrial morphology and function, and adrenergic response in brown adipose tissue. *Journal of Biological Chemistry* 277(45):42958–42963.
- [42] Wu, B.N., O'Sullivan, A.J., 2011. Sex differences in energy metabolism need to be considered with lifestyle modifications in humans. *Journal of Nutrition and Metabolism* 2011:391809.
- [43] Arciero, P.J., Goran, M.I., Poehlman, E.T., 1993. Resting metabolic rate is lower in women than in men. *Journal of Applied Physiology* (1985) 75(6):2514–2520.
- [44] Kaikaew, K., Grefhorst, A., Visser, J.A., 2021. Sex differences in Brown adipose tissue function: sex hormones, glucocorticoids, and their crosstalk. *Frontiers in Endocrinology* 12:652444.
- [45] Varlamov, O., Bethea, C.L., Roberts Jr., C.T., 2014. Sex-specific differences in lipid and glucose metabolism. *Frontiers in Endocrinology* 5:241.
- [46] Foley, J.E., Kashiwagi, A., Chang, H., Huecksteadt, T.P., Lillioja, S., Verso, M.A., et al., 1984. Sex difference in insulin-stimulated glucose transport in rat and human adipocytes. *American Journal of Physiology* 246(3 Pt 1):E211–E215.
- [47] Macotela, Y., Boucher, J., Tran, T.T., Kahn, C.R., 2009. Sex and depot differences in adipocyte insulin sensitivity and glucose metabolism. *Diabetes* 58(4):803–812.
- [48] Corsetti, J.P., Sparks, J.D., Peterson, R.G., Smith, R.L., Sparks, C.E., 2000. Effect of dietary fat on the development of non-insulin dependent diabetes mellitus in obese Zucker diabetic fatty male and female rats. *Atherosclerosis* 148(2):231–241.
- [49] Trevasik, J.L., Meyer, E.A., Galgani, J.E., Butler, A.A., 2008. Counterintuitive effects of double-heterozygous null melanocortin-4 receptor and leptin genes on diet-induced obesity and insulin resistance in C57BL/6J mice. *Endocrinology* 149(1):174–184.
- [50] Patil, M., Sharma, B.K., Elattar, S., Chang, J., Kapil, S., Yuan, J., et al., 2017. Id1 promotes obesity by suppressing Brown adipose thermogenesis and white adipose browning. *Diabetes* 66(6):1611–1625.
- [51] Hunter, C.S., Rhodes, S.J., 2005. LIM-homeodomain genes in mammalian development and human disease. *Molecular Biology Reports* 32(2):67–77.
- [52] de Jong, J.M., Larsson, O., Cannon, B., Nedergaard, J., 2015. A stringent validation of mouse adipose tissue identity markers. *American Journal of Physiology. Endocrinology and Metabolism* 308(12):E1085–E1105.
- [53] Lindroos, J., Husa, J., Mitterer, G., Haschemi, A., Rauscher, S., Haas, R., et al., 2013. Human but not mouse adipogenesis is critically dependent on LMO3. *Cell Metabolism* 18(1):62–74.
- [54] Sun, Y., Geng, M., Yuan, Y., Guo, P., Chen, Y., Yang, D., et al., 2020. Lmo4-resistin signaling contributes to adipose tissue-liver crosstalk upon weight cycling. *The FASEB Journal* 34(3):4732–4748.
- [55] Tsai, J., Tong, Q., Tan, G., Chang, A.N., Orkin, S.H., Hotamisligil, G.S., 2005. The transcription factor GATA2 regulates differentiation of brown adipocytes. *EMBO Reports* 6(9):879–884.
- [56] Emont, M.P., Yu, H., Wu, J., 2015. Transcriptional control and hormonal response of thermogenic fat. *Journal of Endocrinology* 225(2):R35–R47.
- [57] Visvader, J.E., Mao, X., Fujiwara, Y., Hahm, K., Orkin, S.H., 1997. The LIM-domain binding protein Ldb1 and its partner LMO2 act as negative regulators of erythroid differentiation. *Proceedings of the National Academy of Sciences of the U S A* 94(25):13707–13712.
- [58] Xu, Z., Huang, S., Chang, L.S., Agulnick, A.D., Brandt, S.J., 2003. Identification of a TAL1 target gene reveals a positive role for the LIM domain-binding protein Ldb1 in erythroid gene expression and differentiation. *Molecular and Cellular Biology* 23(21):7585–7599.
- [59] de Melo, J., Clark, B.S., Venkataraman, A., Shiau, F., Zibetti, C., Blackshaw, S., 2018. Ldb1- and Rnf12-dependent regulation of Lhx2 controls the relative balance between neurogenesis and gliogenesis in the retina. *Development* 145(9).
- [60] Terano, T., Zhong, Y., Toyokuni, S., Hiai, H., Yamada, Y., 2005. Transcriptional control of fetal liver hematopoiesis: dominant negative effect of the over-expression of the LIM domain mutants of LMO2. *Experimental Hematology* 33(6):641–651.
- [61] van Meyel, D.J., O'Keefe, D.D., Jurata, L.W., Thor, S., Gill, G.N., Thomas, J.B., 1999. Chip and apterous physically interact to form a functional complex during *Drosophila* development. *Molecular Cell* 4(2):259–265.
- [62] Xiao, D., Jin, K., Xiang, M., 2018. Necessity and sufficiency of Ldb1 in the generation, differentiation and maintenance of non-photoreceptor cell types during retinal development. *Frontiers in Molecular Neuroscience* 11:271.